Remote Sensing Applications: Society and Environment 27 (2022) 100812

Contents lists available at ScienceDirect

Remote Sensing Applications: Society and Environment

journal homepage: www.elsevier.com/locate/rsase

Crop classification based on phenology information by using time series of optical and synthetic-aperture radar images

Fatemeh Kordi [a], Hossein Yousefi [b,*]

[a] Department of Remote Sensing and GIS, Faculty of Geography, University of Tehran, Tehran, Iran
[b] Faculty of New Sciences and Technologies, University of Tehran, Tehran, Iran

ARTICLE INFO

Keywords:
Agricultural products
Optic
Phenology
Radar
Support vector machine
TIMESAT model

ABSTRACT

Crop classification provides essential information for ensuring global food security, allowing early crop monitoring practices and water irrigation management. Despite of high importance of satellite imagery in identifying agricultural products, a significant number of optical images could become inaccessible due to cloud cover, which makes mapping agricultural products difficult. Therefore, the provision of up-to-date data integration methods and the availability of time series of optical and radar images such as Sentinel-1 data have provided new opportunities for mapping agricultural products with high spatial and temporal resolution. In this study, the results of classification accuracy were investigated based on the phenology of agricultural products and using time series of Landsat 8, Sentinel-1 and the digital elevation model (DEM). To do so, the key phenological parameters of the products such as start of season, length of season and end of season were first extracted using time series of the NDVI vegetation index calculated from the optical images and the TIMESAT model. Then, based on vegetation phenology of crops using optical (Landsat-8) and radar (Sentinel-1) time series data along with Digital Elevation Model (DEM) to increase the accuracy of classification, we applied the support vector machine method based on machine learning. The performance of this model was investigated on a part of Miandoab catchment basin located in the catchment of Lake Urmia in the northwest of Iran. Also, five major agricultural products of the study area, such as alfalfa, wheat, sugar beet, apple and grape were identified with overall accuracy of 89% using the support vector machine algorithm. Classification results demonstrated that using a combination of different data (overall accuracy (OA) = 89%, Kappa = 0.78) were more accurate than the only single-sensor inputs (OA = 77%, Kappa = 0.64), and when differences between crop types were largest, classification performance increased throughout the season until July.

Abbreviations

%	Percent
DEM	Digital Elevation Model
NDVI	Normalized Difference Vegetation Index
EVI	Enhanced Vegetation Index
LAI	Leaf Area Index

* Corresponding author.
E-mail addresses: kordi.fatemeh@ut.ac.ir (F. Kordi), Hosseinyousefi@ut.ac.ir (H. Yousefi).

https://doi.org/10.1016/j.rsase.2022.100812
Received 16 June 2022; Received in revised form 11 July 2022; Accepted 12 July 2022
Available online 19 July 2022

GNDVI	Green Normalized Difference Vegetation Index
VV	Vertical Vertical
VH	Vertical Horizontal
MSI	Multi Spectral Instrument
SAR	Synthetic Aperture Radar
OLI	Operational Land Imager
ETM^{+}	Enhanced Thematic Mapper Plus
TM	Thematic Mapper
EMISAR	Electro Magnetics Institute Synthetic Aperture Radar
ERS	European Remote-Sensing Satellite
SVM	Support Vector Machine
MLC	Maximum Likelihood Classification
DT	Decision Trees
NN	Neural Network
ULRP	Urmia Lake Restoration Program
GRD	Ground Range Detected
SRTM	Shuttle Radar Topography Mission
GLCM	Gray-Level Co-Occurrence Matrix
OA	Overall Accuracy
Ce	Commission Error
Oe	Omission Error
PA	Producer Accuracy
UA	User Accuracy

1. Introduction

In the future, more agricultural products will be needed to provide food (Foley et al., 2011). In addition, biofuel production and urban growth will increase the pressure on the agricultural sector (Godfray et al., 2010). All of these factors will have consequences for natural ecosystems (Green et al., 2005). Knowledge about types of agricultural products can help managers and farmers to apply appropriate management and executive policies to determine the type of cultivation specific to each region, estimate the potential for harvesting, manage agricultural lands in accordance with local needs and conditions, manage water resources (Demarez et al., 2019). A map of crop sequences can be produced by combining information from multiple years, thus providing an indicator of agricultural land use intensity. Both duration and diversity of crop sequences are directly related to landscape complexity (Tscharntke et al., 2021).

One of the effective tools for monitoring, studying, and determining types of agricultural products is satellite data (Van Tricht et al., 2018). Remote sensing techniques are widely used in all sectors including agriculture due to their ability to provide update data and high image analysis (Bégué et al., 2018). In Iran, estimation of the area under cultivation of various agricultural products is usually made through three methods: expert estimation, estimation through cataloging, and the use of remote sensing and GIS (Kenduiywo et al., 2018). Studies have shown that the accuracy of the first and second methods is very low and they have many errors (Ziaeian-Firoozabadi et al., 2009).Therefore, it is necessary to use more accurate, faster, and less expensive methods to promote various macro-planning, including agriculture (Nirbhay Bhuyar, 2020). Biophysical parameters, including fresh and dry weight and leaf area index can also be obtained using vegetation indices calculated from Landsat 8 OLI and Landsat 7 ETM+ (Ahmadian et al., 2016).

However, in spite of potential of optical remote sensing data in crop classification, there are some questions about where meteorological conditions can affect the behavior of the optical signal especially in cloud condition. Similarly, even though SAR remote sensing is a good choice to overcome a part of the meteorological conditions, its potential to gain information on the physical characteristics and structure of crop is still unknown for the identification and characterization in detail of cloud condition crop patterns (Carrasco et al., 2019).

Research has suggested that full-polarization radar data are needed to achieve high-quality results in mapping crop types, but other researchers have come to different conclusions based on their experience. Moreover, although the use of reflection coefficients has an overall accuracy (OA) less than 50% (Roychowdhury, 2020), more accurate classification is possible using the combination of haralic textures, the VV/VH polarization ratio, and the local mean with VV reflection coefficients (Inglada et al., 2016).

Combination of optical data (Sentinel-2 or Landsat 8) and SAR data, such as Sentinel-1 data could improve the identification and differentiation between crops type, whose detection is difficult using only optical images (Vuolo et al., 2018). By combining optical, SAR, and environmental data, overall accuracy was increased by 6%–10% compared to single-sensor approaches, where optical data performed better than SAR. The mapped areas corresponded well to agricultural statistics at a regional and national level, and their accuracy ranged between 78% and 80% (Blickensdörfer et al., 2022).

Agricultural products mapping in different climates and cultivation systems using optical time series are presented (Sonobe et al., 2018). However, optical images affected by cloud cover reduce the performance of these images in mapping agricultural products. Some studies have shown that the phenological properties of agriculture products obtained from optical sensors are also useful for

estimating the area under crop (Zhang et al., 2017). Therefore, to achieve this goal, combining optical and radar time series data could be a smart method due to the regular revisit times and the independence of radar images from weather conditions. Further studies have examined the suitability of X- and C-band SAR data to determine the growth stages of rice (Yuzugullu et al., 2017).

Likewise, the multi-temporal classification method has been demonstrated in several studies using a combination of optics and radar time series data (Larrañaga and Álvarez-Mozos, 2016). Most methods used to classify agricultural products have used all available data during the growing season, regardless of vegetation phenology of agricultural products (Skriver, 2012). Although these studies have yielded significant results on the classification of agricultural products, a number of them have encountered difficulties in distinguishing and identifying some products such as cereals (Bargiel and Herrmann, 2011). Therefore, knowledge about vegetation phenology of crops can play a decisive role in improving the results of agricultural products classification (Bargiel, 2017).

Furthermore, examining the views related to the production of agricultural products maps, it was concluded that it is not possible to accurately classify them by selecting images related to specific dates and all available data should be used (Inglada et al., 2016). However, in a study, using the Electro Magnetics Institute Synthetic Aperture Radar (EMISAR) airborne system showing monthly polarimetric data at 20% error rate in some areas, they could use the images taken at the most appropriate and optimal time for mapping agricultural products (Skriver, 2012). In another study, using multi-temporal ERS-1 data, 12 crops were separated with 80% accuracy (Schotten et al., 1995).To achieve this goal, they needed to choose the best images from 14 available im-ages during the agricultural season. Moreover, in a similar study, only two Sentinel-1 images were used to identify some land uses(Balzter et al., 2015).

In addition to good quality remote sensing data, classification algorithms are necessary to produce accurate maps of agricultural products. Based on multi-temporal NDVI curves, the RF and SVM classifiers performed better than the SAM classifier in identifying crops (Ouzemou et al., 2018). For example, in one study, four methods of supervise classification such as support vector machine classification (SVMs), decision trees (DTs), neural network classification, and maximum likelihood classification (MLC) were analyzed on Landsat TM data. Results showed that support vector machine (SVMs) outperformed the other three algorithms (Huang et al., 2007).

This study aims to assess the potential of optical (Landsat-8) and radar (Sentinel-1) time series data along with DEM for crop classification based on vegetation phenology when optimal remote sensing data are not available due to atmospheric effects such as cloud and haze contamination. The case study considered in this article is located in the northwestern part of Iran. To classify agricultural products, the support vector machine method based on machine learning algorithm was applied. Finally, the results of the classification were validated using ground data collected in 2014. The main reason for selecting the year 2014 was the availability of ground truth data fo this year in order to validation of the results of classification.

1.1. Study area

The location of the study area has been shown in Fig. 1. Miandoab plain, with an area of 438,000 ha in the northwestern part of Iran, forms a large part of western Miandoab, which is one of the suitable areas for agricultural production downstream of Lake Urmia

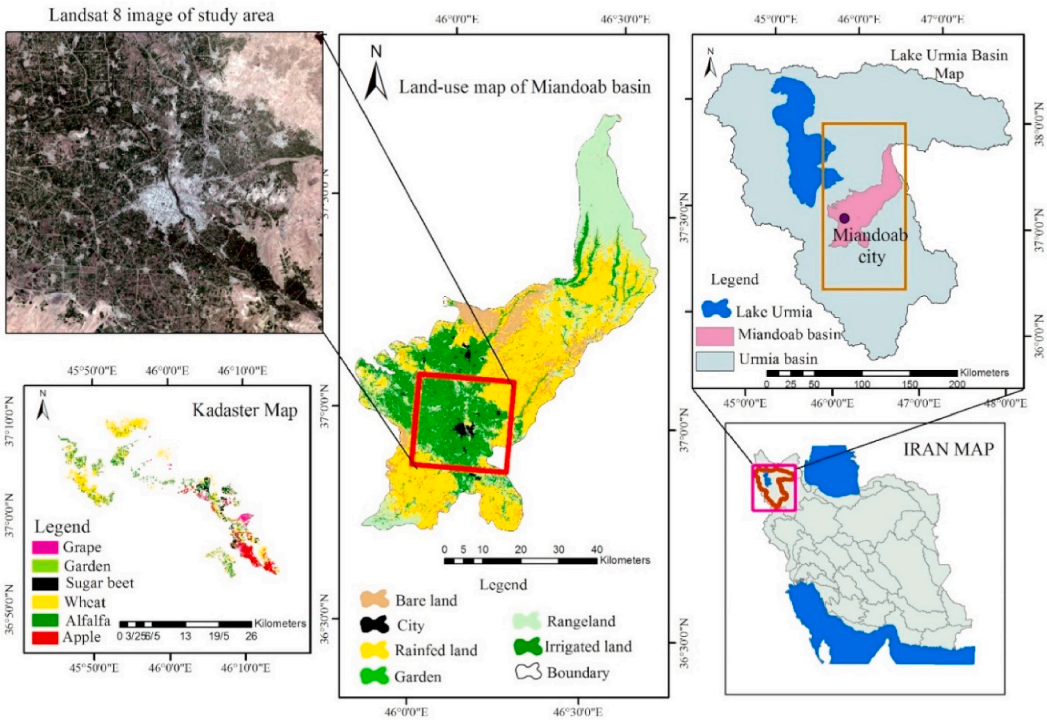

Fig. 1. Geographic location of study area in northwestern Lake Urmia, Iran.

catchment due to its favorable climate. The geographical coordinates of the study area is from 45° 43′ 11″ to 46° 50′ 42″ east longitude and from 36° 40′ 49″ to 37° 44′ 2″ north latitude. This region has a cold and semi-arid cold climate according to Umberg classification and a cold semi-arid climate according to De Martonne classification. The annual rainfall in the study area is about 254 mm.

1.2. Reference dataset

To evaluate and validate the results, ground truth data are of great importance along with satellite data. In this study, this data included information about the crop calendar, land harvested points, and cadastral map. In Fig. 2, a few of the points and cadastral data retrieved from Google Earth are shown with area photos taken during the field visit. In the study area, the Urmia Lake Restoration Program (ULRP) and Novinabyari website provided most of the ground truth data during the growth period.

The ground truth data collected in this study were related to the 2014–2015 crop years and no data were available for the subsequent years. Therefore, since the Sentinel-2A was launched in June 2015, firstly, these images did not cover the growing season of the products in the desired years. Secondly, it was not possible to validate the results without ground data. Table 1 shows the area of major agricultural products in the study area and the percentages of these lands in relation to the total agricultural lands in the Miandoab catchment area. The number of points used in the classification were 18500, to avoid training data imbalances that might negatively affect the SVM algorithm, 50% training samples and 50% validation samples were used for each land-use classification.

1.3. Satellite data

The Landsat8 satellite was successfully launched in February 2013. This satellite uses OLI as well as infrared thermal sensors. Also, Landsat 8 have ability to acquire images from the surface of the earth with a spatial resolution of 30 m and a temporal resolution of 16 days, as a georeference likewise other satellites of the Landsat series. Each image frame obtained from the Landsat 8 satellite can cover an area, which is 170 km north-south wide and 183 km east-west long (Zanter, 2016). In the present study, processed Landsat 8 images of Level 2A (atmospherically corrected surface reflectance by masking clouds, cloud shadows, water, and snow) were used. The study area was covered by one Landsat 8 image frame. All Landsat 8 images were resampled by Cubic Convolution to 10 m to be combined with radar images (Torres et al., 2012). According to the study time, radar images of Sentinel-1 (Interferometric Wide Swath mode) with a 12-day revisit time were used. Currently, the revisit time is in the range of 3–6 days depending on the combination of S1-A and S1–B platforms. In Sentinel-1, synthetic aperture radar (SAR) data has been acquired in the C-band for a dual-polarization system. There are three resolutions (10, 25, or 40m) and four bands (corresponding to scene polarization) available in Sentinel-1 data. These images were taken with a spatial resolution of 10 m with a constant incidence angle in VV and VH polarizations. All images were Level 1-GRD (Ground Range Detected) and radiometric and orthorectified corrections were applied on them using SNAP software. Then, From the two original bands, two new bands were calculated as (VV + VH) and (VH/VV). Lee 3 filter was also used to reduce the speckle noise. The acquisition date of Landsat8 and Sentinel-1A images has been shown in Table 2. It should be also noted that Iota2 software was used to fill temporal gap of cloud pixels (Inglada et al., 2015). The used gap-filling model relied on linear interpolation. Moreover, masked cloud pixels were estimated by linear interpolation using pixel information of the images taken of a date after and a date before when it was not cloudy. Therefore, a Landsat-8 image became available every 16 days. Since different agricultural products

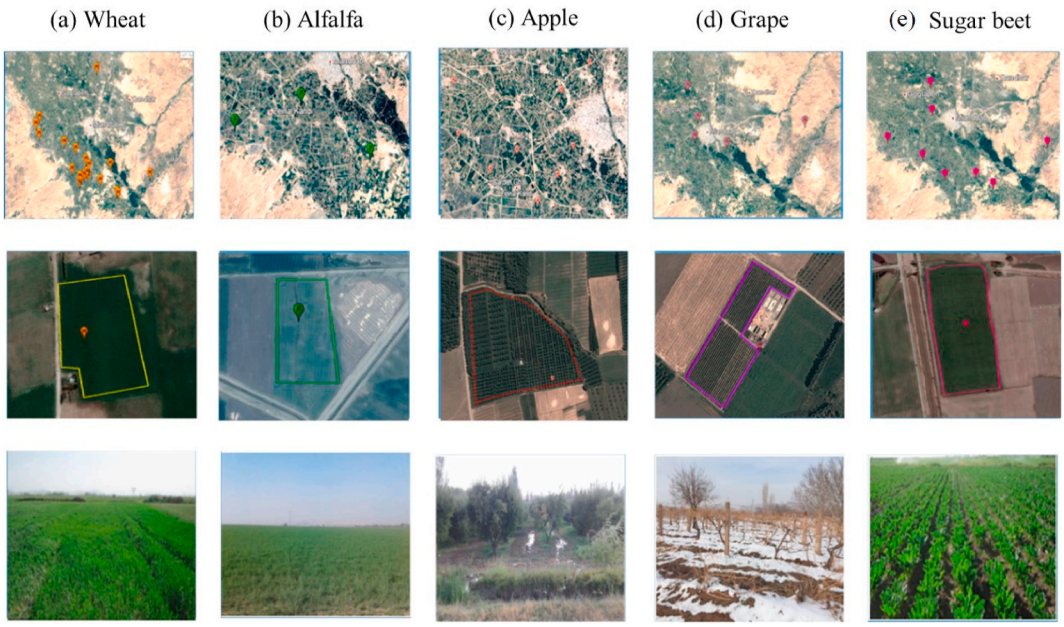

Fig. 2. The figures of (a), (b), (c), (d) and (e) illustrates ground truth points and cadaster on Google Earth of wheat, Alfalfa, apple, grape and sugar beet respectively, also the photos of agriculture land which are taken during growing season in the study area has shown.

Table 1
Overview of ground truth data for the vegetation season 2014/2015.

Land cover	Total area (ha)	Percentage to total area	Number of ground truth
Alfalfa	12566	73.12	4800
Sugar beet	6269	35.6	2500
Wheat	25179	51.25	3500
Apple	16251	46.16	3500
Grape	11280	43.11	3000
Other Gardens	235	24	1200

Table 2
Dates of Landsat 8 and Sentinel-1 data acquisition for the study area.

Dates of Landsat-8 imagery			Dates of Sentinel-1 imagery		
Year	Month	Day	Year	Month	Day
2014	April	8; 24	2015	April	3
	May	10; 26		July	8
	June	11; 27		August	1; 25
	July	13; 29	2016	April	3
	August	14; 30		July	2; 14
	September	15		August	19
	October	1; 17		September	18
2015	April	11; 27			
	May	13; 29			
	June	14; 30			
	July	16			
	August	1; 17			
	September	2; 18			
	October	4; 20			
2016	April	13; 29			
	May	15; 31			
	June	16			
	July	2; 18			
	August	3; 19			
	September	4; 20			
	October	6; 22			

are grown at different elevation, therefore, the effect of SRTM Digital Elevation Model with a spatial resolution of 30 m on classification was evaluated.

2. Materials and methods

In Fig. 3, the flowchart of the general implementation process of the study is shown. In this study, it was tried to identify and classify the agricultural products of the study area by using time series of optical and radar images. This goal was achieved through several stages. Firstly, the images of the Landsat8 satellite images with a spatial resolution of 30 m and the Sentinel-1 satellite images with a spatial resolution of 10 m were downloaded and processed. Secondly, various vegetation indices were calculated using Landsat8 images for the studied years. Then, the key phenological parameters were extracted using the TIMESAT model. Finally, the agricultural products of the study area were classified using the support vector machine algorithm. To train and evaluate the obtained results, the ground truth data (cadaster and harvested land points) of the study area were used.

2.1. Extraction of vegetation phenological information

In some studies, various vegetation indices have been used to extract phenological parameters. In the present study, to find the most effective vegetation indices, four vegetation indices, including normalized difference vegetation index (NDVI), enhanced vegetation index (EVI), leaf area index (LAI), and green normalized difference vegetation index (GNDVI) were evaluated.

Vegetation indices for the cultivation period (seven months) of 2014, 2015, and 2016 were also calculated and the trend of crop changes in these indices was examined. Table 3 summarizes VIs that are sensitive to changes in vegetation cover and plant health conditions and have been used to improve land coverage classification and crop mapping accuracy in similar studies. Fig. 4 shows the vegetation indices calculated for date of 29 July 2014 image of Landsat8.

Furthermore, the time series of vegetation indices were obtained from satellite spectral measurements to analyze the structural and functional characteristics of land cover. To put in another way, this indices can be used to determine the necessary information about seasonal changes in vegetation. Today, there are a limited number of methods for detecting and extracting the variability of time series data. One of these models is the TIMESAT model developed to extract oscillating parameters (Eklundha and Jönsson, 2017). Three methods available in TIMESAT are performed based on the least squares fitting and the highest numerical value of the vegetation index. The first method is based on local polynomial functions known as the Savitzky-Golay adaptive filter, a digital filter that can be

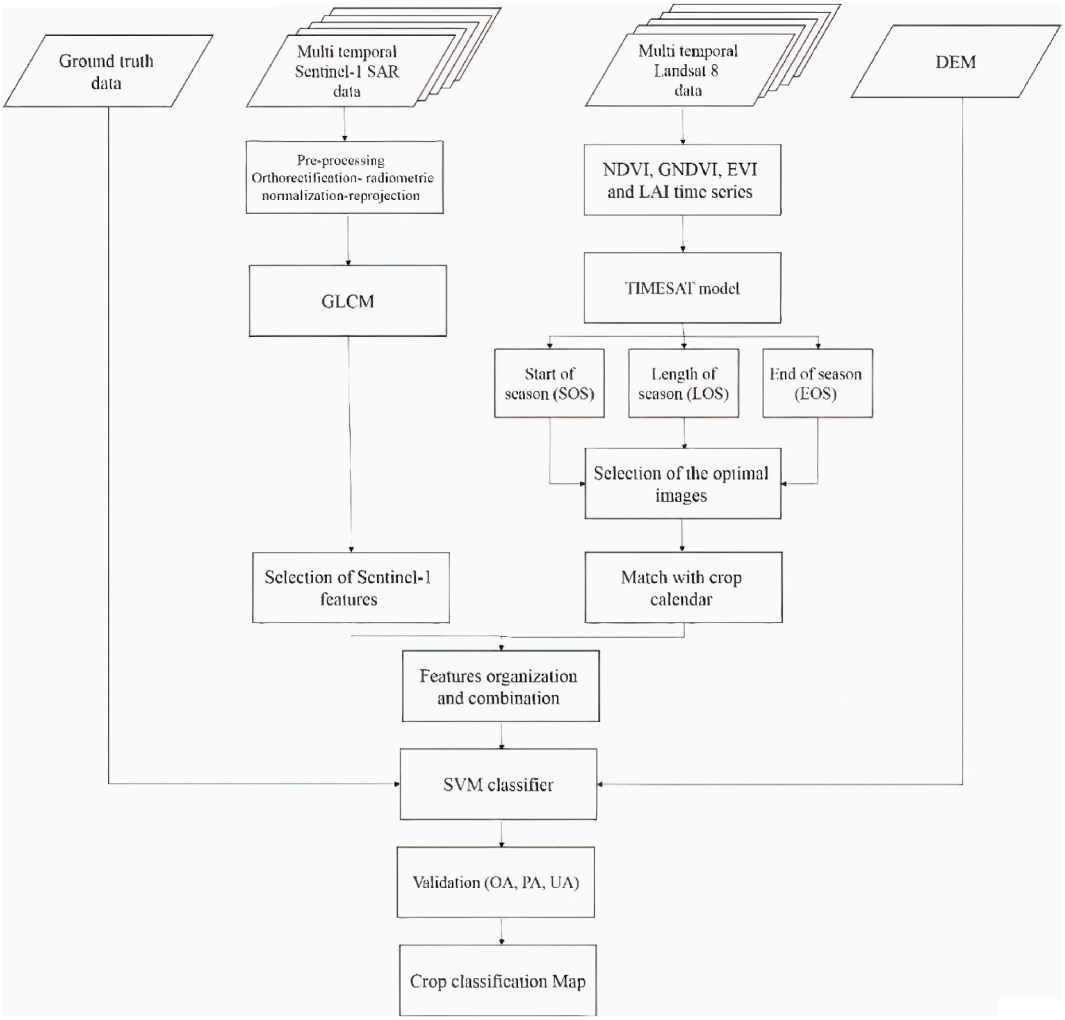

Fig. 3. Flowchart of crop classification map based phenology information using time-series of optical and SAR data.

Table 3
The vegetation indices computed in this study from the Landsat 8.

Name	Formula	Reference
NDVI	$NDVI = \frac{\rho(NIR) - \rho(R)}{\rho(NIR) + \rho(R)}$	Rousel et al. (1973)
EVI	$EVI = \left(\frac{P^*_{NIR} - P^*_{RED}}{P^*_{NIR} + C_1 P^*_{RED} - C_2 P^*_{BLUE} + 1}\right)_{1+L}$	Huete (1988)
LAI	$LAI = -\frac{\ln\left(\frac{0.69 - SAVI_{ID}}{0.59}\right)}{0.91}$	Bastiaanssen et al. (2000)
GNDVI	$GNDVI = \frac{\rho(NIR) - \rho(G)}{\rho(NIR) + \rho(G)}$	Gitelson et al. (1996)

applied to a set of points to smooth the data. The other two methods, asymmetric Gaussian and double logistics, fit information with complex nonlinear functions. All these three processing methods use a preliminary definition of the actual growing season (unimodal or bimodal) along with the approximate time of the growing season (Eklundha and Jönsson, 2017). Studies (Jensen and Lulla, 1987) indicate that Savitzky-Golay method is not always successful in finding good results when applied to uneven time series (with high fluctuations). An asymmetric Gaussian or double logistics model may be more appropriate in such cases. It has been shown in recent studies (Inglada et al., 2016) that NDVI provides useful information about agricultural patterns in images with high spatial and temporal resolution. In order to achieve this, the double logistic model, which is modeled in Eq. (1) will be used in the present study (Eklundha and Jönsson, 2017).

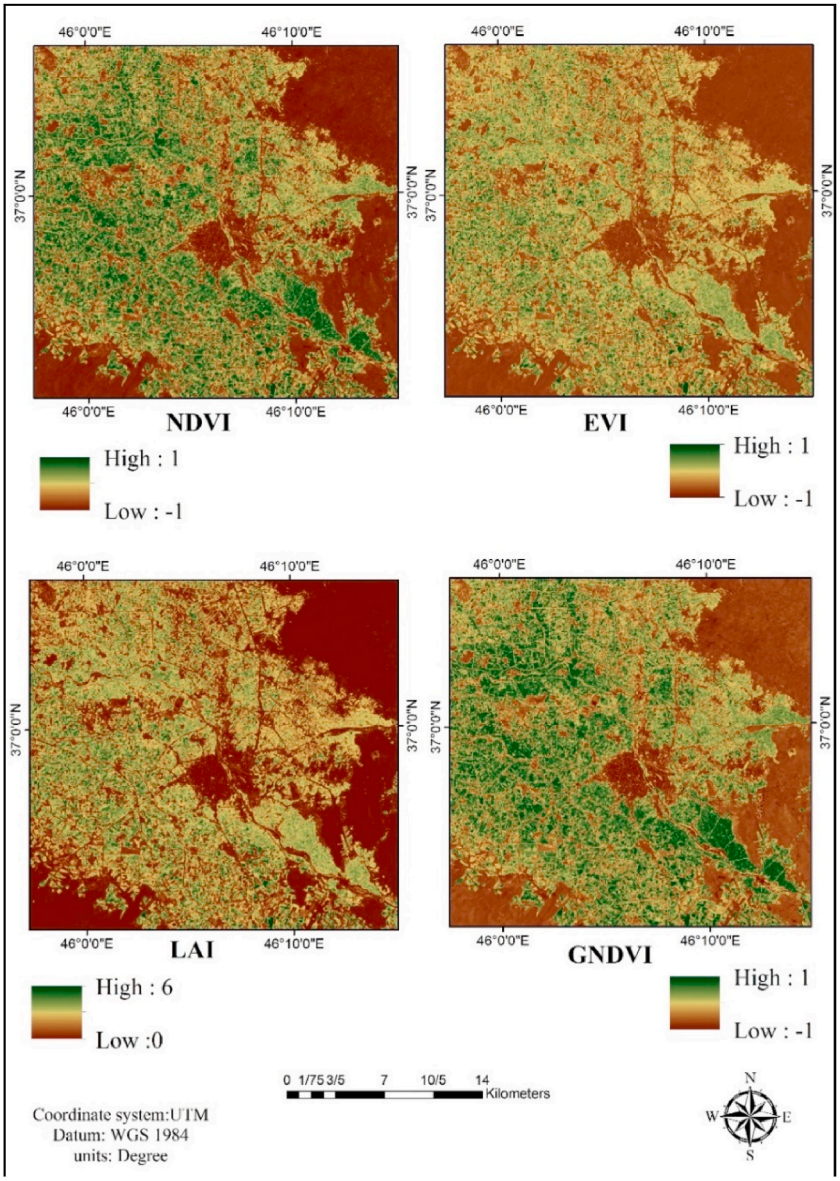

Fig. 4. Vegetation indices for 29 July 2014 image of Landsat-8.

Eq. (1) was applied to the vegetation index of NDVI calculated from Landsat8 images. In Eq. (1), x_1 determines the position of the left inflection point while x_2 gives the rate of change. Similarly x_3 determines the position of the right inflection point while x4 gives the rate of change at this point. Also for this function the parameters are restricted in range to ensure a smooth shape.

$$g(t;x_1,\ldots,x_4)=\frac{1}{1+\exp\left(\frac{x_1-t}{x_2}\right)}-\frac{1}{1+\exp\left(\frac{x_3-t}{x_4}\right)} \tag{1}$$

TIMESAT model provides key information about plant phenology, such as beginning of growing season, maximum date of growth, date of end of growth, and length of growing season by examining plant phenology during growth period using time series of vegetation indices. Then, the most optimal images can be selected for high-precision classification by matching this information with the crop calendar of the region. Finally, the map of crops is prepared using selected images (based on plant phenology) and training data.

2.2. Definition of phenological stages

The phenological stages of crops occur at different times in the growing season. This process depends on the type of crop, sowing date, climatic conditions, and soil type in the area. The crop calendar of 2014 for each crop varies according to the specific location, the climatic conditions, and the crop year. Fig. 5 shows the crop calendar of major agricultural products in the study area, including wheat,

sugar beet, alfalfa, apples, and grapes. According to the crop calendar in the year 2014 in Miandoab plain, land preparation for cultivation of irrigated wheat begins in mid-September and usually lasts until early December. Also, cultivation time for irrigated wheat is October and November and sometimes lasts until mid-December. Moreover, harvesting this crop starts from early October (after planting and the first irrigation) and lasts until the end of June. In the study area, harvesting irrigated wheat begins in early July and lasts until mid-September. In order to cultivate sugar beet, the land is plowed with a reversible plow from October to late November, and in April, the land is plowed and disked again. Then, the land is leveled using a roller. Planting sugar beet starts in April and continues until early May. Harvesting sugar beet begins in mid-October and lasts until mid-December. In the study area of Miandoab, as for most parts of Iran, alfalfa is cultivated in two seasons of early spring and early autumn and gives 3–4 harvests a year. The first harvest begins in July and the last harvest is usually in October. The operation related to the preparation of apple garden is also performed from early October to late December. This crop is planted and harvested in April and during October, respectively. Furthermore, according to the crop calendar, operations related to the preparation of vineyards are performed from early October to late November. The planting date and harvest time of this crop are also April and the second half of September, respectively.

2.3. Crop-classification using time series data

Generally, information on the classification of agricultural products is obtained from radar images (SAR imagery) with VV polarization, Haralik texture (entropy and inertia calculated from VV polarization), and polarization ratio (VV/VH). In a study, VH polarization as well as entropy and inertia calculated from VH polarity were used (Zhou et al., 2019a). The GLCM is the most widely used method of extracting texture from remote sensing images. This method was proposed by Haralik in 1973, which is a second-order texture index, and it has been used in many studies to increase the accuracy of classification (Zhou et al., 2019b). In this study, the GLCM method was used for extracting texture. In current study, 16 textural matrices are calculated (Conners et al., 1984; Hall-Beyer, 2017). provide more details on the equation of each textural matrix. In another study, using time series images of Landsat 5 (TM) (1995–2005), changes in land use in agricultural lands were investigated by two methods of pixel-based and object-oriented classification. They found that both methods had the same accuracy, except for the object-oriented method having problems, such as not considering small classes and merging them with larger ones, which in turn reduced accuracy (Robertson and King, 2011). In the study area, it is noticed that due to the small area of agricultural land, object-oriented classification did not have high efficiency and accuracy in the separation and segregation of small agricultural land. Therefore, the support vector machine (SVM) method was used as the most effective classification methods that have been widely used with the Gaussian kernel function (Burges, 1998). This method has been introduced as a powerful method in detecting and determining different types of soil along with five agricultural products with an overall accuracy of 92% (Foody and Mathur, 2004). The main reason for using this method and its favorable results in comparison with other classifiers is that SVM algorithm use geometric features of training data instead of statistical features (Karjalainen et al., 2008).

2.4. Validation of results

The use of any kind of thematic information requires knowledge of its correctness and accuracy. Each classification is evaluated and performed using reference datasets, which are randomly divided into two parts: 50% of ground truth data is used for training, while the other 50% is used for validation of results. In the present study, the coefficients of overall accuracy, Kappa coefficient, producer accuracy, user accuracy, Omission error, and Commission error were used to check the classification accuracy. A detailed explanation of the equation of overall accuracy and the kappa coefficient can be found in (Jensen, 1986).

3. Results and discussion

3.1. Investigating the trend of changes in vegetation index

Using the coordinates of the existing land points, the trend of changes in agricultural products in the study area was separately investigated in the calculated vegetation indices. As mentioned earlier, the main agricultural products of the region included: apples,

Fig. 5. Crop calendar for agriculture products in the study area.

grapes, alfalfa, wheat, sugar beet, and various orchards. The trend of changes in orchard class and apple were close to each other and due to the fact that these crops are tree-type and have high greenery during the growing period, they had higher values in terms of the studied vegetation indices compared to other products. In addition, these crops had more peaks during their growth period due to their different phenological stages, such as leaf production, flowering, and fruit production. On the other side, there were no fluctuations in the process of changing vineyards and its maximum growth occurred in July. In addition, according to the diagram drawn for grapes, this crop was harvested in late August. In the case of crops such as alfalfa, the maximum growth occurred in 31st August which is shown in Fig. 6. Alfalfa is also one of the crops in the study area that is planted and harvested two to three times a year; therefore, its growth trends can be completely variable from one year to the next. Beginning in June, wheat was entered the growing stage, reaching its peak by the end of July. Additionally, sugar beet has a longer growth period than other crops due to the way it is processed. In Fig. 6, the trend of changes in NDVI in the study area is shown for each crop during the cultivation period.

3.2. TIMESAT model

The trend of phenological changes of the studied crops with more focus on parameters, such as the beginning of crops season, the end of crops season, and the length of crops season was obtained from the TIMESAT model. Results of this model were adapted to the crop calendar. Since the TIMESAT model is able to detect n-1 seasons and considering that the time series data of the present study were related to three years (2014, 2015, and 2016), the model was able to determine two seasons or two cultivation periods; therefore, the results of 2014 were used considering the available ground truth data in the present study. In addition, by reviewing the results of the performance of indices and the adaptation of the outputs obtained from the TIMESAT model with the crop calendar, the most efficient index among vegetation indices was selected. According to the results of TIMESAT model, although the results of the four vegetation indices were closely related, the NDVI's phenological parameters were more closely related to the crop calendar; thus, this index was used for mapping crops. Table 4 shows the results of the TIMESAT model derived from the NDVI.

According to the information obtained from the TIMESAT model and the crop calendar of agricultural products in the study area in 2014, the dates of cultivation and harvest of grapes are April and the second half of September, respectively. The crop calendars of apple and grape, which fall into the horticultural category are very close to each other. Moreover, the operation related to the preparation of apple land is performed from late September to late November. The planting date of this product is April and its harvest is done from September 22 to October 11. Furthermore, in the study area, the crop calendar of horticultural crops, including plum, cherry, etc., is similar to apple orchards and very close to each other so that like apple, their land preparation operations is performed from late September to late November. The planting date of these crops is April and their harvest is done from September 22nd, 2014 to October 11th, 2014. On the other side, alfalfa is known as a spring-autumn crop, whose land preparation operations start from late February to early April. The planting date of this product is from 1st to 10th April. Indeed, alfalfa is harvested twice when 10% of the whole field alfalfa has the flowering stage. Harvesting this product includes three stages of cutting, collecting, and packing. In the study area, alfalfa is harvested three times with an almost 45-day interval. In Miandoab, the first harvest of alfalfa is performed around the end of June and the last harvest is performed in late September. In addition, wheat is an autumn crop, whose land preparation operation is from late August to early October. Planting date of this product is from October 2nd to October 22nd. The best time to harvest wheat is when the grains have a moisture content of about 14%. Depending on the planting date, this stage starts from around the end of June in the study area. Considering sugar beet, it is a spring crop, whose land is prepared from late February to the first decade of April. The planting date of this crop is April 10th to April 20th. Also, harvesting of sugar beet begins when its old leaves turn yellow and the growth of young leaves inside the plant slows down (reduction of growth of aerial organs). In Miandoab, the date of harvesting sugar beet has been scheduled for the first half of September. Fig. 7 illustrates the plant's phenological development for major crops in the study area.

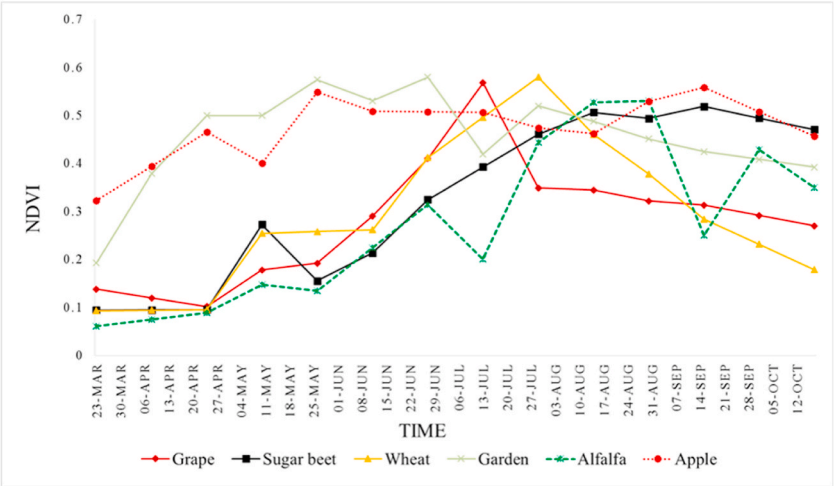

Fig. 6. Changes trend of NDVI for agriculture products in 2014.

Table 4
Extraction of key phonological parameters for agriculture products from NDVI time series using TIMESAT model.

Input TIMESAT model	Agriculture Products	Start of season	Maximum growth	End of season
NDVI	Grape	10 May 2014	30 Aug 2014	1 Oct 2014
	Apple	8 Apr 2014	29 Jul 2014	1 Oct 2014
	Wheat	16 Apr 2014	18 May 2014	19 Jun 2014
	Garden	8 Apr 2014	27 Jun 2014	30 Aug 2014
	Alfalfa	11 Jun 2014	29 July 2014	1 Oct 2014
	Sugar beet	27 Jun 2014	30 Sep 2014	17 Oct 2014

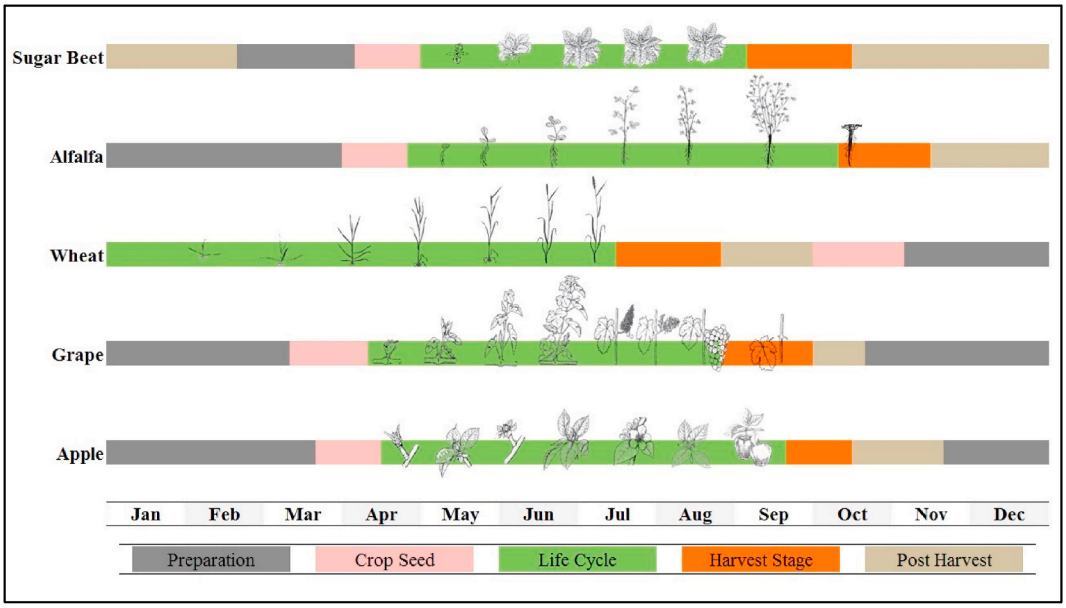

Fig. 7. Plant's phenological stages for agriculture products in Miandoab, Images of plants are taken from (Meier, 1997).

In the current study, by comparing the results of the TIMESAT model and examining the phenological trend for the five products, it can be concluded that each plant has the most changes at certain times during its growth period. These changes are more obvious at three time intervals, including the beginning of the season (April 8th and May 10th), when the plant reaches its maximum growth (June 27th and August 30th), and the end of the season (September 18th and October 1st) than other stages of the plant growth period. Therefore, by examining the phenological efficiency of plants, the classification algorithm was run using the selected images obtained from the TIMESAT model shown in Table 5. The use of selected images not only accelerated the classification process, but also it improved the classification results (see Table 6).

3.3. *Evaluating the accuracy of results*

After the classification operation, its results were quantitatively estimated by comparing the classified map with the ground reality and using accuracy criteria. The result of this evaluation is presented in the form of a confusion matrix (Jensen and Lulla, 1987). In the confusion matrix, the reference data (matrix columns) were compared with the classification data (matrix rows). In fact, correctly classified pixels were placed in the diameter of the table and non-diagonal pixels had not been classified properly. The confusion matrix obtained from the SVM method is given in Table 5. Moreover, Kappa coefficient and the overall accuracy for the classified map were estimated to be 0.88 and 89%, respectively. Overall accuracy is a measure of the accuracy of classification. One of the limitations of

Table 5
Date of optimal Images for Classification.

Year	Month	Day
2014	April	8
	May	10
	June	27
	August	30
	September	18
	October	1

overall accuracy is that pixels that have been erroneously assigned to a class as well as pixels that have not been classified into their actual class are not taken into account (Jensen and Lulla, 1987). The kappa coefficient is the same as the overall accuracy criterion; however, because the kappa coefficient considers the incorrectly classified pixels, it is better than the overall accuracy criterion. The accuracy of UA and PA classification for each crop is shown in Table 7. It is also clear that the accuracy of classifying each crop individually is higher than the overall classification accuracy of the whole map. In general, the classification accuracy of alfalfa, apple, and wheat classes is higher than others. Also, due to the fact that the garden class may be a combination of several different products, it has a lower classification accuracy than other classes.

The classification map of crops is given in Fig. 8. As shown in Fig. 8, the five major crops of the study area (wheat, sugar beet, alfalfa, apple, and grape) can be well-distinguished from each other using optical and radar time series data. Further, each color on the map represents a crop; for example, red color on the map shows the area under apple cultivation and the yellow, light blue, and green areas show the area under wheat, alfalfa, and orchards, respectively. Also, purple, black, and gray represent the class of grapes, sugar beets, and non-agricultural lands, respectively.

In a number of fields in the study area, alfalfa crop is planted first and after harvesting alfalfa (in July of the same year), sugar beet and wheat crops are still in the growth and greening stage. Therefore, on these lands, there are crop and green cover throughout the spring and summer. In addition, due to the presence of more weeds in May than in September, there is a possibility that more fallow lands would be mistakenly considered as wheat and alfalfa crops. However, in this study, the use of radar satellite data played a decisive role in eliminating such errors, increasing the accuracy of classification by 10%, and better separation of different crops due to their sensitivity to the shape and size of crops and the study of plant phenology. Classification results demonstrated that using a combination of different data (Optical and SAR) (overall accuracy (OA) = 89%, Kappa = 0.78) were more accurate than the only single-sensor inputs (OA = 77%, Kappa = 0.64), and when differences between crop types.

In this paper, a crop classification map was presented to differentiate and identify crops types using Landsat 8 and Sentinel-1 time series data and digital elevation model in agricultural areas based on plant phenological changes during the growing season (Chong et al., 2021). found that using time-series images is significantly more accurate than using single-period images, since time-series images show spectral information and phenological characteristics that contribute to better crop classification. However, the accuracy of some months, in particular May and October, was better than others. Winter and summer are the transitional months between the two seasons. As most of the cultivated lands are herbaceous crops, this could be unique to this study area (Nabil et al., 2022).

A map achieved with overall accuracy of 89% and a Kappa coefficient of 0.78 when Landsat 8 spectral bands, DEM and vegetation indices were stacked with Radar monthly polarization bands. The results are slightly better than those based solely on Sentinel-1 bands and indices, but a significant improvement over those based solely on Sentinel-1 bands.

Tree-fruit classification was influenced by Sentinel-1 polarization channels. In tree crop discrimination, Sentinel-1 VH cross-polarization played a crucial role. Since the VH is extremely sensitive to changes in vegetation phenology, it can be widely used to extract phonological information from vegetation (Stendardi et al., 2019), Increasing the accuracy of crop classification(Chakhar et al., 2021).

Phenological identification in satellite images has been done in order to improve the classification of agricultural products based on the TIMESAT model. Classification based on plant phenology focuses on different growth stages, such as the beginning of the growing season, the maximum growth, the length of the growing season, and the end of the season for each crop. It was found that spectral similarity between deciduous species reduced the accuracy of separability, and if there is a noticeable phenological difference between species, segregation of species would be more desirable. In the current investigation, the result presented that by examining the spectral reflectance of major crops (wheat, sugar beet, grapes, alfalfa and apples) based on the time series of satellite images as well as the results obtained from applying vegetation index on each image, the area under cultivation of crops according to the type of cultivation and the cultivation pattern cannot be extracted by using only a single image. In other words, spectral similarity of crops in the study area was the main reason for the inefficiency of an image in separating different agricultural products. Each phenological stage of a crop contains specific information that makes it possible to distinguish the products from each other. Therefore, according to the processing performed on the time series of NDVI, the optimal dates were identified using the TIMESAT model. Finally, classification was performed using optical and radar images through the SVM method. Therefore, by focusing on data, whose date is optimally determined based on the TIMESAT model, more accurate classification results can be achieved. Furthermore, the use of SVM classification algorithm in classifying crops provides relatively good results due to its high flexibility for different conditions and purposes. It should be also noted that determining the optimal conditions in this method is of great importance. Whereas the results demonstrate the performance of Landsat 8 and Sentinel-1 individually, they also emphasize that classification using the Landsat8 dataset always outperformed that using the Sentinel-1 dataset. The effect of elevation on classification accuracy is significant until late May, while it is not after that. In this study, the use of DEM significantly affected the early stages of crop growth, but when the crops reached their final stages of full growth, DEM was not significant. Also, the Sentinel-1 images alone did not perform well in the detection and segregation of agricultural products, but the combination of these images with optical and DEM data significantly increased the accuracy of the results. Therefore, to develop a robust method, which is applicable over time and in large areas, it is necessary to use radar data which are not dependent on weather conditions unlike optical data. In fact, this study evaluated the respective advantages of using a combination of Optical and SAR parameters with OA ranging from 89% (Kappa = 0.78). Meanwhile, it is very important to prepare a product map and know the type of cultivation pattern in a region, because by knowing a region's cultivation pattern, it is possible to eliminate those products having high water consumption and lower yields. The optimal cultivation pattern can be obtained according to the area conditions. For example, crops with high water consumption and resistant to drought and salinity, such as sorghum and sesame can be used considering that water wastage in Iran and many countries is higher than the global average and the agricultural sector has been introduced as the largest consumer of water in many countries. As a result, knowing the pattern of cultivation is the

Table 6
Confusion matrix of SVM classification (%).

Crop types	Alfalfa	Sugar beet	Wheat	Apple	Grape	Gardens
Alfalfa	88.6	7.1	6.4	0.1	0.1	2.4
Sugar beet	10.2	88.3	1.2	0	0.7	0
Wheat	0.9	4.4	92.1	0	0	0
Apple	0.3	0	0	88.1	5.8	13.2
Grape	0	0.2	0.3	3.2	87.3	3.9
Gardens	0	0	0	8.6	6.1	80.5

Table 7
Producer's accuracies (PA) and user's accuracies (UA) achieved by SVM classifier.

class	PA	UA
Alfalfa	88.62	95.91
Sugar beet	88.35	90.32
Wheat	92.14	77.15
Apple	88.11	95.12
Grape	87.37	78.54
Gardens	80.50	68.95

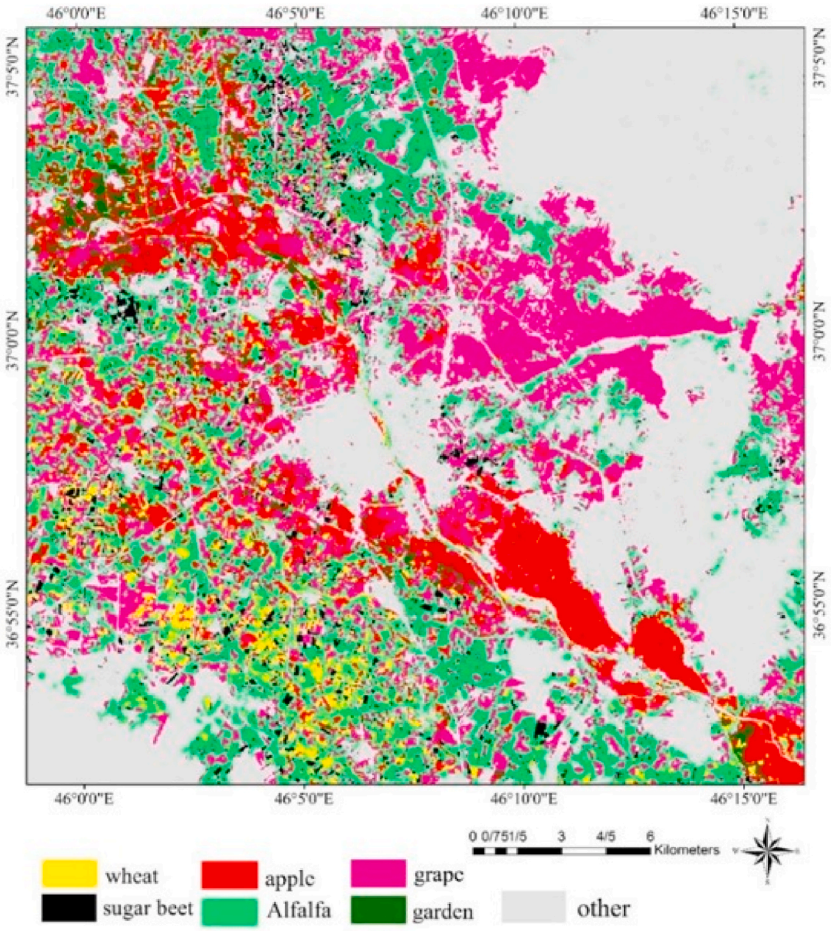

Fig. 8. Crop classification map of the study area, during the growing season 2014–2015.

most important method to reduce agricultural water consumption and develop the agricultural area.

4. Conclusion

This study was conducted to improve the accuracy in classification results based on crops phenology obtained from combining the time series of optical and radar data with the digital elevation model. The results showed that combining Sentinel-1 and Landsat 8 data improved classification accuracy compared to the case performed with only optical or radar images. The use of radar data limits the use of temporal gap-filled models to generate interpolated data from other images for filling masked cloud pixels. This in turn increases the accuracy of classification results. This method can also determine the type of products in very large areas under different climatic conditions. It was found that using optimal time series Landsat 8 spectral bands and vegetation indices could yield a high level of classification accuracy (89%), whereas using Sentinel-1 polarization channels with added textural features could result in a high level of classification accuracy (77%). The Kappa coefficient and overall accuracy were estimated 0.78 and 89% for the crops map classified by support vector machine. The results of this study also showed that satellite images had a high capability for segregation of crops and preparation of crop-type maps as well as maps of area under cultivation with appropriate accuracy at the regional scale. Therefore, satellite data could be applied in the agricultural sectors, such as forecasting and estimating damage, plant stress, drainage status, and so on. In addition, in order to stabilize the market, maps of cultivation of crops in the region can be used for many cases, including surveying statistics of the region and remotely determining the type of product, calculating the area under cultivation of crops in the region, estimating the number of machines required for cultivation of different crops in the region, determining the amount of net production, as well as the amount of shortage or surplus of agricultural products. According to our results, it is suggested to use our developed method to prepare a map for different agricultural products with different images and sensors in other areas.

Ethical statement for solid state ionics

Hereby, I/Hossein Yousefi/consciously assure that for the manuscript/Crop classification based on phenology information by using time series of optical and Synthetic-aperture radar images for optimizing management of water resources/the following is fulfilled:

1) This material is the authors' own original work, which has not been previously published elsewhere.
2) The paper is not currently being considered for publication elsewhere.
3) The paper reflects the authors' own research and analysis in a truthful and complete manner.
4) The paper properly credits the meaningful contributions of co-authors and co-researchers.
5) The results are appropriately placed in the context of prior and existing research.
6) All sources used are properly disclosed (correct citation). Literally copying of text must be indicated as such by using quotation marks and giving proper reference.
7) All authors have been personally and actively involved in substantial work leading to the paper, and will take public responsibility for its content.

The violation of the Ethical Statement rules may result in severe consequences.

To verify originality, your article may be checked by the originality detection software iThenticate. See also http://www.elsevier.com/editors/plagdetect.

I agree with the above statements and declare that this submission follows the policies of Solid State Ionics as outlined in the Guide for Authors and in the Ethical Statement.

Author statement

Fatemeh Kordi: conceived and designed the Conceptualization, methodology, software, validation visualization and writing the draft preparation.

Hossein Yousefi: Contributed to the writing, review and editing and supervision the paper.

Declaration of competing interest

The authors declare that they have no known competing financial interests or personal relationships that could have appeared to influence the work reported in this paper.

Acknowledgments

The authors would like to appreciate the Urmia Lake Restoration Program (ULRP) and Ministry of Jihad Agriculture (Deputy of Water and Soil) for providing the ground truth data used in this research.

References

Ahmadian, N., Ghasemi, S., Wigneron, J.P., Zölitz, R., 2016. Comprehensive study of the biophysical parameters of agricultural crops based on assessing Landsat 8 OLI and Landsat 7 ETM+ vegetation indices. GIScience Remote Sens. 53, 337–359. https://doi.org/10.1080/15481603.2016.1155789.

Balzter, H., Cole, B., Thiel, C., Schmullius, C., 2015. Mapping CORINE land cover from Sentinel-1A SAR and SRTM digital elevation model data using random forests. Rem. Sens. 7, 14876–14898.

Bargiel, D., 2017. A new method for crop classification combining time series of radar images and crop phenology information. Remote Sens. Environ. 198, 369–383. https://doi.org/10.1016/j.rse.2017.06.022.

Bargiel, D., Herrmann, S., 2011. Multi-temporal land-cover classification of agricultural areas in two European regions with high resolution spotlight TerraSAR-X data. Rem. Sens. 3, 859–877. https://doi.org/10.3390/rs3050859.
Bastiaanssen, W.G.M., Molden, D.J., Makin, I.W., 2000. Remote sensing for irrigated agriculture: examples from research and possible applications. Agric. Water Manag. 46, 137–155. https://doi.org/10.1016/S0378-3774(00)00080-9.
Bégué, A., Arvor, D., Bellon, B., Betbeder, J., de Abelleyra, D., Ferraz, R.P.D., Lebourgeois, V., Lelong, C., Simões, M., Verón, S.R., 2018. Remote sensing and cropping practices: a review. Rem. Sens. 10, 1–32. https://doi.org/10.3390/rs10010099.
Bhuyar, Nirbhay, 2020. Crop classification with multi-temporal satellite image data. Int. J. Eng. Res. V9 https://doi.org/10.17577/ijertv9is060208.
Blickensdörfer, L., Schwieder, M., Pflugmacher, D., Nendel, C., Erasmi, S., Hostert, P., 2022. Mapping of crop types and crop sequences with combined time series of Sentinel-1, Sentinel-2 and Landsat 8 data for Germany. Remote Sens. Environ. 269, 112831.
Burges, C.J.C., 1998. A tutorial on support vector machines for pattern recognition. Data Min. Knowl. Discov. 2, 121–167. https://doi.org/10.1023/A:1009715923555.
Carrasco, L., O'Neil, A.W., Daniel Morton, R., Rowland, C.S., 2019. Evaluating combinations of temporally aggregated sentinel-1, sentinel-2 and Landsat 8 for land cover mapping with Google earth engine. Rem. Sens. 11 https://doi.org/10.3390/rs11030288.
Chakhar, A., Hernández-López, D., Ballesteros, R., Moreno, M.A., 2021. Improving the accuracy of multiple algorithms for crop classification by integrating sentinel-1 observations with sentinel-2 data. Rem. Sens. 13, 243.
Chong, L.U.O., Liu, H., Lu, L., Liu, Z., Kong, F., Zhang, X., 2021. Monthly composites from Sentinel-1 and Sentinel-2 images for regional major crop mapping with Google Earth Engine. J. Integr. Agric. 20, 1944–1957.
Conners, R.W., Trivedi, M.M., Harlow, C.A., 1984. Segmentation of a high-resolution urban scene using texture operators. Comput. Vis. Graph Image Process 25, 273–310.
Demarez, V., Helen, F., Marais-Sicre, C., Baup, F., 2019. In-season mapping of irrigated crops using Landsat 8 and Sentinel-1 time series. Rem. Sens. 11, 118. https://doi.org/10.3390/rs11020118.
Eklundha, L., Jönsson, P., 2017. TIMESAT 3.3 with Seasonal Trend Decomposition and Parallel Processing Software Manual.
Foley, J.A., Ramankutty, N., Brauman, K.A., Cassidy, E.S., Gerber, J.S., Johnston, M., Mueller, N.D., O'Connell, C., Ray, D.K., West, P.C., Balzer, C., Bennett, E.M., Carpenter, S.R., Hill, J., Monfreda, C., Polasky, S., Rockström, J., Sheehan, J., Siebert, S., Tilman, D., Zaks, D.P.M., 2011. Solutions for a cultivated planet. Nature 478, 337–342. https://doi.org/10.1038/nature10452.
Foody, G.M., Mathur, A., 2004. A relative evaluation of multiclass image classification by support vector machines. IEEE Trans. Geosci. Rem. Sens. 42, 1335–1343. https://doi.org/10.1109/TGRS.2004.827257.
Gitelson, A.A., Kaufman, Y.J., Merzlyak, M.N., 1996. Use of a green channel in remote sensing of global vegetation from EOS-MODIS. Remote Sens. Environ. 58, 289–298.
Godfray, H.C.J., Beddington, J.R., Crute, I.R., Haddad, L., Lawrence, D., Muir, J.F., Pretty, J., Robinson, S., Thomas, S.M., Toulmin, C., 2010. Food security: the challenge of feeding 9 billion people. Science. https://doi.org/10.1126/science.1185383.
Green, R.E., Cornell, S.J., Scharlemann, J.P.W., Balmford, A., 2005. Farming and the fate of wild nature. Science 307, 550–555. https://doi.org/10.1126/science.1106049.
Hall-Beyer, M., 2017. Practical guidelines for choosing GLCM textures to use in landscape classification tasks over a range of moderate spatial scales. Int. J. Rem. Sens. 38, 1312–1338. https://doi.org/10.1080/01431161.2016.1278314.
Huang, X., Zhang, L., Li, P., 2007. Classification and extraction of spatial features in urban areas using high-resolution multispectral imagery. Geosci. Rem. Sens. Lett. IEEE 4, 260–264. https://doi.org/10.1109/LGRS.2006.890540.
Huete, A.R., 1988. A soil-adjusted vegetation index (SAVI). Remote Sens. Environ. 25, 295–309.
Inglada, J., Arias, M., Tardy, B., Hagolle, O., Valero, S., Morin, D., Dedieu, G., Sepulcre, G., Bontemps, S., Defourny, P., Koetz, B., 2015. Assessment of an operational system for crop type map production using high temporal and spatial resolution satellite optical imagery. Rem. Sens. 7, 12356–12379. https://doi.org/10.3390/rs70912356.
Inglada, J., Vincent, A., Arias, M., Marais-Sicre, C., 2016. Improved early crop type identification by joint use of high temporal resolution SAR and optical image time series. Rem. Sens. 8, 362. https://doi.org/10.3390/rs8050362.
Jensen, J.R., 1986. Introductory Digital Image Processing: a Remote Sensing Perspective. Univ. of South Carolina, Columbus.
Jensen, J.R., Lulla, K., 1987. Introductory digital image processing: a remote sensing perspective. Geocarto Int. 2, 65. https://doi.org/10.1080/10106048709354084.
Karjalainen, M., Kaartinen, H., Hyyppä, J., 2008. Agricultural monitoring using envisat alternating polarization SAR images. Photogramm. Eng. Rem. Sens. 74, 117–126. https://doi.org/10.14358/PERS.74.1.117.
Kenduiywo, B.K., Bargiel, D., Soergel, U., 2018. Crop-type mapping from a sequence of Sentinel 1 images. Int. J. Rem. Sens. 39, 6383–6404. https://doi.org/10.1080/01431161.2018.1460503.
Larrañaga, A., Álvarez-Mozos, J., 2016. On the added value of quad-pol data in a multi-temporal crop classification framework based on RADARSAT-2 imagery. Rem. Sens. 8, 335. https://doi.org/10.3390/rs8040335.
Meier, U., 1997. Growth Stages of Mono- and Dicotyledonous Plants. Blackwell Wissenschafts-Verlag.
Nabil, M., Farg, E., Arafat, S.M., Aboelghar, M., Afify, N.M., Elsharkawy, M.M., 2022. Tree-fruits crop type mapping from Sentinel-1 and Sentinel-2 data integration in Egypt's New Delta project. Remote Sens. Appl.: Soc. Environ., 100776
Ouzemou, J.E., El Harti, A., Lhissou, R., El Moujahid, A., Bouch, N., El Ouazzani, R., Bachaoui, E.M., El Ghmari, A., 2018. Crop type mapping from pansharpened Landsat 8 NDVI data: a case of a highly fragmented and intensive agricultural system. Remote Sens. Appl.: Soc. Environ. 11, 94–103. https://doi.org/10.1016/j.rsase.2018.05.002.
Robertson, L.D., King, D.J., 2011. Comparison of pixel-and object-based classification in land cover change mapping. Int. J. Rem. Sens. 32, 1505–1529. https://doi.org/10.1080/01431160903571791.
Rousel, J., Haas, R., Schell, J., Deering, D., 1973. Monitoring vegetation systems in the great plains with ERTS. In: Proceedings of the Third Earth Resources Technology Satellite—1 Symposium, pp. 309–317. NASA SP-351.
Roychowdhury, K., 2020. Comparison between spectral, spatial and polarimetric classification of urban and periurban landcover using temporal SENTINEL-1 images. https://doi.org/10.5194/isprsarchives-XLI-B7-789-2016.
Schotten, C.G., Van Rooy, W.W., Janssen, L.L., 1995. Assessment of the capabilities of multi-temporal ers-1 sar data to discriminate between agricultural crops. Int. J. Rem. Sens. 16, 2619–2637. https://doi.org/10.1080/01431169508954580.
Skriver, H., 2012. Crop classification by multitemporal C- and L-band single- and dual-polarization and fully polarimetric SAR. IEEE Trans. Geosci. Rem. Sens. 50, 2138–2149. https://doi.org/10.1109/TGRS.2011.2172994.
Sonobe, R., Yamaya, Y., Tani, H., Wang, X., Kobayashi, N., Mochizuki, K., 2018. Crop classification from Sentinel-2-derived vegetation indices using ensemble learning. J. Appl. Remote Sens. 12, 1. https://doi.org/10.1117/1.jrs.12.026019.
Stendardi, L., Karlsen, S.R., Niedrist, G., Gerdol, R., Zebisch, M., Rossi, M., Notarnicola, C., 2019. Exploiting time series of Sentinel-1 and Sentinel-2 imagery to detect meadow phenology in mountain regions. Rem. Sens. 11, 542.
Torres, R., Snoeij, P., Geudtner, D., Bibby, D., Davidson, M., Attema, E., Potin, P., Rommen, B.Ö., Floury, N., Brown, M., Traver, I.N., Deghaye, P., Duesmann, B., Rosich, B., Miranda, N., Bruno, C., L'Abbate, M., Croci, R., Pietropaolo, A., Huchler, M., Rostan, F., 2012. GMES Sentinel-1 mission. Remote Sens. Environ. 120, 9–24. https://doi.org/10.1016/j.rse.2011.05.028.
Van Tricht, K., Gobin, A., Gilliams, S., Piccard, I., 2018. Synergistic use of radar sentinel-1 and optical sentinel-2 imagery for crop mapping: a case study for Belgium. Rem. Sens. 10, 1–22. https://doi.org/10.3390/rs10101642.
Tscharntke, T., Grass, I., Wanger, T.C., Westphal, C., Batáry, P., 2021. Beyond organic farming–harnessing biodiversity-friendly landscapes. Trends Ecol. Evol. 36, 919–930.

Vuolo, F., Neuwirth, M., Immitzer, M., Atzberger, C., Ng, W.T., 2018. How much does multi-temporal Sentinel-2 data improve crop type classification? Int. J. Appl. Earth Obs. Geoinf. 72, 122–130. https://doi.org/10.1016/j.jag.2018.06.007.

Yuzugullu, O., Erten, E., Hajnsek, I., 2017. Estimation of rice crop height from X-and C-band PolSAR by metamodel-based optimization. IEEE J. Sel. Top. Appl. Earth Obs. Rem. Sens. 10, 194–204. https://doi.org/10.1109/JSTARS.2016.2575362.

Zanter, K., 2016. Landsat 8 (L8) Data Users Handbook, Landsat Science Official Website. US Geological Survey, Reston, VA, USA.

Zhang, H., Li, Q., Liu, J., Shang, J., Du, X., Zhao, L., Wang, N., Dong, T., 2017. Crop classification and acreage estimation in North Korea using phenology features. GIScience Remote Sens. 54, 381–406. https://doi.org/10.1080/15481603.2016.1276255.

Zhou, Y., Luo, J., Feng, L., Zhou, X., 2019a. DCN-based spatial features for improving parcel-based crop classification using high-resolution optical images and multi-temporal SAR data. Rem. Sens. 11, 1619.

Zhou, Y., Luo, J., Feng, L., Zhou, X., 2019b. DCN-based spatial features for improving parcel-based crop classification using high-resolution optical images and multi-temporal SAR data, 2019 Rem. Sens. 11. https://doi.org/10.3390/RS11131619, 1619 11, 1619.

Ziaeian-Firoozabadi, P., Sayad-Bydhndy, L., Eskandari-Nodeh, M., 2009. Mapping and estimating the area under rice cultivation in Sari city using satellite images Radarst. Goegraph. Res. Nat. 68, 45–58.